LITERATURE CITED

Aris, R., "A Normalization for the Thiele Modulus," *Ind. Eng. Chem. Fund.*, **4**, 227 (1965).

Bischoff, K. B., "Effectiveness Factors for General Reaction Rate Forms," *AIChE J.*, **11**, 351 (1965).

Butt, J. B., D. M. Downing, and J. W. Lee, "Inter-Intraphase Temperature Gradients in Fresh and Deactivated Catalyst Particles," *Ind. Eng. Chem. Fund.*, **16**, 270 (1977).

Carberry, J. J., "On the Relative Importance of External-Internal Temperature Gradients in Heterogeneous Catalysis," *ibid.*, **14**, 129 (1975).

——, *Chemical and Catalytic Reaction Engineering*, Chapt. 9, McGraw-Hill, New York (1976).

Downing, D. M., J. W. Lee, and J. B. Butt, "Simulation Models for Intraparticle Deactivation: Scope and Reliability," *AIChE J.*, **25**, 461 (1979).

Foster, R. N., J. B. Butt, and H. Bliss, "Diffusional Mass Transport of Nonadsorbed Gases within Porous Structures," *J. Catal.*, **7**, 179 (1964).

Froment, G. F., and K. B. Bischoff, *Chemical Reactor Analysis and Design*, Chapt. 2, John Wiley & Sons, New York (1979).

Kehoe, J. P. G., and J. B. Butt, "Kinetics of Benzene Hydrogenation by Supported Nickel at Low Temperature," *J. Appl. Chem. Biotechnol.*, **22**, 23 (1972).

Lee, J. W., J. B. Butt, and D. M. Downing, "Kinetic, Transport and Deactivation Rate Interactions on Steady State and Transient Responses in Heterogeneous Catalysis," *AIChE J.*, **24**, 212 (1978).

Lee, J. W., "Effects of Intraparticle Deactivation on Catalyst Performance," Ph.D. dissertation, Northwestern University, Evanston, IL (1976).

Petersen, E. E., "A General Criterion for Diffusion Influenced Chemical Reactions in Porous Solids," *Chem. Eng. Sci.*, **20**, 587 (1965).

Wheeler, A., "Reaction Rates and Selectivity in Catalyst Pores," *Adv. in Catal.*, **2**, 249 (1955).

Manuscript received October 24, 1980; revision received April 20 and accepted July 14, 1981.

Part II. Design and Analysis: Approach of Reactor Point Effectiveness

A design method is presented that takes into account the effects of both diffusion and deactivation on heterogeneous catalytic reactors. Improvements that can be made by the method are demonstrated and an efficient methodology is developed by which the design problem as well as associated optimization problems can be solved in a routine manner. The approach is based on the reactor point effectiveness for global rate of reaction in terms of bulk fluid conditions. Some important features emerge from the examples presented.

HONG H. LEE

Department of Chemical Engineering
University of Florida
Gainesville, FL 32611

JOHN B. BUTT

Department of Chemical Engineering
and
Ipatieff Catalytic Laboratory
Northwestern University
Evanston, IL 60201

SCOPE

Heterogeneous catalytic reactors are usually designed on the basis of initial catalyst activity, even when deactivation is known to occur, and compensation made via subsequent operating conditions. An exception is the work of Weekman (1968) on catalytic cracking of gas oil affected by coking. In the present paper a design practice including the effect of catalyst deactivation is presented to demonstrate the improvements possible by such methods. While the problem including both deactivation and diffusion limitation is difficult (particularly so for complex kinetics), it is possible to develop an efficient methodology for solution based on the reactor point effectiveness factor for global rate of reaction in terms of bulk conditions.

CONCLUSIONS AND SIGNIFICANCE

If the effect of catalyst deactivation on reactor operation is included in the design phase, improvements in performance can be obtained that are not possible with the usual design practice based on the activity of fresh catalyst. In fact, decisions based on the latter method can lead to incorrect conclusions regarding reactor performance. The proposed methodology here allows routine solution for heterogeneous catalytic reactors affected by diffusion and either uniform or pore-mouth deactivation. The procedure can also be used for the optimization of an operating reactor.

INTRODUCTION

Very little attention has been directed to the design and analysis problem of heterogeneous catalytic reactors subject to the double jeopardy of diffusion limitation and catalyst deactivation. The work of Dumez and Froment (1976) is among the very few in which both deactivation and diffusion are treated within the context of a heterogeneous reactor model. Studies employing pseudo homogeneous models have been reported by Froment and Bischoff (1961) for coking, and by Butt and coworkers (1975, 1977) for independent poisoning. These later workers have also studied the behavior of individual catalyst pellets affected by both diffusion and deactivation (1975, 1979).

Usual design practices for heterogeneous reactors are normally

ISSN 0001-1541-82-5586-0410-$2.00. © The American Institute of Chemical Engineers, 1982.

based on fresh catalyst parameters and deactivation is taken into consideration usually only in the form of operating policies that are in some sense optimal. There may be several reasons for this situation; certainly one can be lack of quantitative characterization of the deactivation, either as to mechanism or kinetics or both, during the design phase. However, often much is known, and what remains to be shown is a concrete demonstration that improvements can be made in performance by considering deactivation-diffusion in the primary design. Further, this should be accomplished without undue complication. The complete analysis of a heterogeneous reactor subject to diffusion and deactivation using a two phase model and realistic kinetics is no simple task, as demonstrated by Dumez and Froment. When this is added to some optimization of the design, the numerical analysis often becomes the problem rather than the design.

In this paper we present a method based on the reactor point effectiveness (Lee, 1981) defining the global reaction rate at any point in terms of bulk conditions. This permits transformation of the two-phase model into a simpler pseudohomogeneous one and considerably streamlines the design/analysis required. The reactor point effectiveness employed is based on the pellet effectiveness developed in Part I for the cases of uniform and pore-mouth deactivation.

DESIGN PROBLEM

Consider the problem of specifying the size of a reactor (or related quantities such as volume of catalyst) in which the catalyst activity decreases with time on stream because of deactivation. The mode of operation envisioned requires that the catalyst be regenerated when conversion drops to some specified level at which point the time-on-stream is t_f. A figure of merit for the design is the total amount of reactant converted up to t_f per unit volume of the reactor, and we wish to determine the reactor size, or equivalently the residence time τ, to maximize this quantity. Thus the design problem is:

$$\text{Max } J(\tau) = \text{Max} \int_0^{t_f} (C_{\text{in}} - C_{\text{out}})/\tau \, dt \tag{1}$$

subject to possible constraints on operating conditions such as maximum allowable catalyst temperature and, most importantly, subject to the equations describing the system. For a reactor with countercurrent cooling:

$$\frac{dC_o}{dz} = -\tau \mathrm{R} \quad z \in (0,1) \tag{2}$$

$$\frac{dT_o}{dz} = \frac{(-\Delta H)}{\rho C_p}\tau R + \frac{(\rho C_p)_c}{\rho C_p}\frac{\tau_c}{\tau}\frac{dT_c}{dz} \tag{3}$$

$$-\frac{dT_c}{dz} = \frac{Ua}{(\rho C_p)_c}\tau_c (T_o - T_c) \tag{4}$$

and

$$\frac{dN_o}{dz} = -\tau R_p \tag{5}$$

For an individual catalyst pellet:

$$D\frac{d^2C}{dx^2} = L^2 kg(C)F \quad x \in (0,1) \tag{6}$$

and

$$-\lambda\frac{d^2T}{dx^2} = L^2(-\Delta H)kg(C)F \tag{7}$$

in which the activity factor F obtained in Part I is given by:

$$F = \begin{cases} \sqrt{1-\gamma} & \text{uniform deviation} \quad (8a) \\ \left[\dfrac{(\eta_{\text{ind}})_d(1-\gamma)}{\eta_f}\right]\dfrac{g(C_c)}{g(C_s)} & \text{pore-mouth deactivation} \quad (8b) \end{cases}$$

and:

$$\frac{d\gamma}{dt} = \begin{cases} \dfrac{(k_p)_s N_s}{Q}(1-\gamma) & \text{uniform deactivation} \quad (9a) \\ \dfrac{(k_p)_c}{Q}\left(\dfrac{N_s}{1+(\phi_p)_c^2\gamma}\right) & \text{pore-mouth deactivation} \quad (9b) \end{cases}$$

Concentration and temperature relationships between bulk fluid and pellet surface are given by:

$$h(T_s - T_o) = (-\Delta H)RL \tag{10}$$

$$k_g(C_o - C_s) = RL \tag{11}$$

$$(k_g)_p(N_o - N_s) = R_p L \tag{12}$$

The global rate of deactivation, R_p, is given by:

$$R_p = (k_p)_s N_s(1-\gamma) \quad \text{uniform deactivation} \tag{13a}$$

$$R_p = Dp\left.\frac{dN}{dx}\right|_{x=1} = \frac{(k_p)_c N_s}{1+(\phi_p)_c^2\gamma} \quad \text{pore-mouth deactivation} \tag{13b}$$

with: $D_p\, d^2N/dx^2 = 0$ for $0 \le x \le x_c$ in the latter case. The intrinsic rate for the main reaction is expressed as $kg(C)$, and subscripts o, s and c respectively denote quantities at bulk fluid conditions, pellet surface conditions and at the interface in the pore-mouth deactivated pellet between fresh and deactivated portions. All quantities are defined in the Notation.

While the problem posed can be solved numerically in principle, given the kinetics $kg(C)$, in practice this is not so simple (Eigenberger and Butt, 1976). To simplify matters we will develop a reactor point effectiveness based on the pellet effectiveness of Part I.

REACTOR POINT EFFECTIVENESS

Define a reactor point effectiveness as:

$$\epsilon = \frac{\text{observed rate}}{\text{intrinsic rate at bulk conditions for fresh catalyst}} \tag{14}$$

It follows from the definition of pellet effectiveness, ϵ_p, that

$$\epsilon = \epsilon_p \frac{k_s g(C_s)}{k_o g(C_o)} \approx \epsilon_p \frac{k_s}{k_o} \tag{15}$$

The assumption of $C_s \approx C_o$ is valid under most realistic conditions where the mass Biot number is of order $10^2 - 10^5$ (Carberry, 1976).

Uniform Poisoning. Using the ϵ_p derived in Part I, we obtain from Eq. 15

$$\epsilon = \frac{[2Dk_o(1-\gamma)]^{1/2}}{Lk_o g_o}\left(\frac{k_s}{k_o}\right)^{1/2}\left[\int_{C_L}^{C_o} g(\alpha)d\alpha\right]^{1/2} \tag{16}$$

with: $g_o \equiv g(C_o)$

The ratio of rate constants can be very well approximated (Lee, 1981) by:

$$\left(\frac{k_s}{k_o}\right)^{1/2} = 1 + \frac{1.2E_a(-\Delta H)\epsilon k_o g_o L}{2R_g T_o^2 h} \tag{17}$$

Combining this with Eq. 16 yields for reaction point effectiveness:

$$\epsilon = \frac{\dfrac{1}{Lg_o}\left(\dfrac{2D}{k_o}\right)^{1/2}[(1-\gamma)I(C_o)]^{1/2}}{1 + \dfrac{1.2E_a(-\Delta H)[2Dk_o]^{1/2}}{2hR_g T_o^2}[(1-\gamma)I_o(C_o)]^{1/2}} \tag{18}$$

where:

$$I(C_o) = \int_{C_L}^{C_o} g(\alpha)d\alpha \tag{18a}$$

In this case reactor point effectiveness is expressed solely in terms of bulk fluid conditions for arbitrary kinetics, $k_o g(C_o)$. Intrapellet isothermality is assumed here, in line with conventional wisdom concerning the relative magnitude of intra- and interphase temperature gradients.

Pore-Mouth Poisoning. While the assumption of isothermality

is serviceable for uniform poisoning, Butt and coworkers (1977, 1978) have shown experimentally that in pore mouth poisoning substantial temperature gradients residue in the outer deactivated shell of the pellet, while the undeactivated core is isothermal. Subsequently, Lee (1980) has shown that these temperature differences are given by (for slab geometry):

$$\Delta T_d = \mathrm{Bi}_h \gamma \Delta T_e \tag{19}$$

$$(\Delta T_c + \Delta T_e) = (1 + \mathrm{Bi}_h \gamma)\Delta T_e \tag{20}$$

where ΔT_d $(= T_c - T_s)$ and ΔT_e $(= T_s - T_o)$ are the temperature differences in pellet shell and external boundary layer, respectively, and Bi_h is the Biot number for heat. From the pellet effectiveness derived in Part I for this case, we obtain reactor point effectiveness as:

$$\epsilon = \frac{D(C_o - C_c)}{k_o g_o L^2 \gamma} \tag{21}$$

where C_c is the solution to:

$$C_o - C_c = \left(\frac{L\gamma}{D}\right)(2Dk_c)^{1/2}\left[\int_{C_L}^{C_c} g(\alpha)d\alpha\right]^{1/2} \tag{22}$$

In order to write k_c in terms of bulk fluid conditions, the ratio of rate constants, (k_c/k_o), is expressed as:

$$\left(\frac{k_c}{k_o}\right)^{1/2} = \exp\left\{\left(\frac{E_a}{2R_g T_o}\right)\left[\frac{1 + \mathrm{Bi}_h\gamma)(T_s/T_o - 1)}{1 + (1 + \mathrm{Bi}_h\gamma)(T_s/T_o - 1)}\right]\right\} \tag{23}$$

where Eqs. 19 and 20 have been used to determine (T_c/T_o). Now, from the interphase heat transfer rate T_s/T_o is given by:

$$T_s/T_o - 1 = \frac{(-\Delta H)RL}{hT_o} = \frac{(-\Delta H)\epsilon k_o g_o L}{hT_o} = \frac{(-\Delta H)D(C_o - C_c)}{hT_o L\gamma} \tag{24}$$

Thus combination with Eq. 23 and subsequent substitution into Eq. 22 gives:

$$C_o - C_c = \left(\frac{L\gamma}{D}\right)(2Dk_o)^{1/2}\left[\int_{C_L}^{C_o} g(\alpha)d\alpha\right]^{1/2} \times \exp\left\{\left(\frac{E_a}{2R_g T_o}\right)\left[\frac{(-\Delta H)D(1 + \mathrm{Bi}_h\gamma)(C_o - C_c)}{hT_o L\gamma + (1 + \mathrm{Bi}_h\gamma)(C_o - C_c)(-\Delta H)(D)}\right]\right\} \tag{25}$$

Here again, quantities are at bulk fluid conditions. An iterative solution of Eq. 25 for C_c, when used in Eq. 21, yields the reactor point effectiveness for pore-mouth deactivation.

Comments on Parameters. Before proceeding to the design problem, it is timely to make a few observations concerning the possible variations in diffusional limitation. The value of the generalized modulus evaluated at bed entrance may be used to determine this. The modulus is defined as:

$$\phi_G = \frac{Lg(C)\sqrt{k(1-\gamma)}}{\left[2D\int_0^C g(\alpha)d\alpha\right]^{1/2}} \tag{26}$$

When the value of this modulus exceeds 3, the reaction can be considered to be diffusion limited and the pellet center concentration, C_L, appearing in the reactor point effectiveness can be set equal to zero. Since the catalyst is most likely to be regenerated when the average value of γ exceeds 0.3, this value may be used as an approximation in Eq. 26. If ϕ_G is less than 3, C_L can be approximated by:

$$C_L \approx C_o/\cosh\,\phi_1 \tag{27}$$

where $\phi_1 = L\sqrt{k_1(1-\gamma)/D}$

and k_1 is the rate constant of a pseudo first-order reaction approximating the kinetics of the main reaction. It has been shown (Lee, 1981) that the integrated value of $g(C)$ is not very sensitive to errors in approximating the true value of C_L.

DESIGN AND ANALYSIS: AN EFFICIENT METHODOLOGY

Uniform Deactivation. With the assumption of negligible external mass transfer resistance, Eq. 5 can be rewritten as:

$$\frac{dN_o}{dz} = -\tau(k_p)_s N_o(1-\gamma) \tag{28}$$

Upon integration, for pseudo steady-state conditions, we obtain:

$$N_o(z,t) = (N_o)_{\mathrm{in}} \exp\{-(k_p)_s\tau(1-\gamma)z\} \tag{29}$$

The global rate of the main reaction, R, follows from the definition of reactor point effectiveness and Eq. 16:

$$R = \epsilon k_o g(C_o) = \frac{\sqrt{2Dk_o}\left[(1-\gamma)\int_0^{C_o} g(\alpha)d\alpha\right]^{1/2}/L}{1 - \dfrac{1.2E_a(-\Delta H)\sqrt{2Dk_o}}{2hR_gT_o^2}\left[(1-\gamma)\int_0^{C_o} g(\alpha)d\alpha\right]^{1/2}} \tag{30}$$

In Eq. 30, C_L has been set to zero for a diffusion-limited main reaction. The reactor design/analysis equations come then from simple combination of Eqs. 29, 30 and 2 and 3. The resulting set is:

$$\left\{\frac{L}{\left[2Dk_o\int_0^{C_o} g(\alpha)d\alpha\right]^{1/2}} - \frac{1.2E_a(-\Delta H)L(1-\gamma)^{1/2}}{2hR_gT_o^2}\right\}dC_o = -\tau(1-\gamma)^{1/2}dz \tag{31}$$

$$N_o = (N_o)_{\mathrm{in}} \exp\{-(k_p)_s\tau(1-\gamma)z\} \tag{29}$$

$$\gamma_j = \gamma_{j-1} + \Delta t\left[\frac{(k_p)_s}{Q}N_o(1-\gamma)\right]_{j-1} \tag{32}$$

$$T_o = T_{\mathrm{in}} - \left(\frac{-\Delta H}{\rho C_p}\right)(C_o - C_{\mathrm{in}}) + \frac{(\rho C_p)_c}{\rho C_p}\left(\frac{\tau}{\tau_c}\right)[(T_c)_{\mathrm{in}} - T_c] \tag{33}$$

where $(T_c)_{\mathrm{in}}$ is the coolant temperature at $z = 1$. In the above, Eq. 32 is the Euler version of Eq. 9a for numerical calculations. The last term of Eq. 33 disappears for adiabatic conditions, allowing direct integration of Eq. 31 in terms of C_o with the aid of Eq. 33. For nonadiabatic conditions Eq. 4 has to be solved along with Eq. 33.

Consider first the adiabatic case. At time $t = 0^+$, $\gamma = 0$, integration of Eq. 31 yields complete information on the reactor. At this condition the left hand side of Eq. 31 is a function of C_o only, since T_o can be expressed in terms of C_o, allowing straightforward integration. With pellet surface temperatures calculated (Eqs. 10 and 30) for $(k_p)_s$, the initial N_o profile can be obtained from Eq. 29, and γ for the next time interval Δt then obtained from Eq. 32. With γ_j known as a function of z, Eq. 31 can then be integrated for $C_o = f(z)$ as follows: Starting with inlet conditions, calculate C_o at the next z position by equating the integrated value of the left hand side of Eq. 31 to the known integrated value of the right hand side, then proceed stepwise in this manner up to $z = 1$. Simpson's method has been found satisfactory for this integration. The procedure is repeated until the final time of interest is attained. Similar methods pertain for the nonadiabatic case, however, Eq. 4 must be solved along with Eq. 33 for T_o. These design procedures are summarized in Table 1.

Pore-Mouth Deactivation. Equation 5 can be integrated with the aid of Eq. 13b to give:

$$N_o(z,t) = (N_o)_{\mathrm{in}} \exp\left[\frac{-(k_p)_c\tau}{1 + (\phi_p)_c^2\gamma}\right] \tag{34}$$

Insertion of the reactor point effectiveness, Eq. 21, in Eq. 2 yields:

$$\frac{dC_o}{dz} = -\frac{\tau D(C_o - C_c)}{L^2\gamma} \tag{35}$$

TABLE 1A. DESIGN EQUATIONS FOR PLUG-FLOW REACTORS: UNIFORM POISONING AND DIFFUSION LIMITATION

$$R(C,T) = kg(C)$$

Nonadiabatic, Nonisothermal Reactors

$$\left\{\frac{L}{\left[2Dk_o\int_0^{C_o} g(\alpha)d\alpha\right]^{1/2}} - \frac{1.2E_a(-\Delta H)L(1-\gamma)^{1/2}}{2hR_gT_o^2}\right\} dC_o = -\tau(1-\gamma)^{1/2}dz \tag{A}$$

$$T_o = T_{in} - \left(\frac{-\Delta H}{\rho C_p}\right)(C_o - C_{in}) + \frac{(\rho C_p)_c}{\rho C_p}\frac{\tau}{\tau_c}[(T_c)_{in} - T_c] \tag{B}$$

$$N_o = (N_o)_{in}\exp\{-(k_p)_s\,\tau(1j-\gamma)z\} \tag{C}$$

$$\gamma_j = \gamma_{j-1} + \Delta t\left[\frac{(k_p)_s}{Q}N_o(1-\gamma)\right]_{j-1} \tag{D}$$

$$\epsilon k_o g_o = \frac{(1-\gamma)^{1/2}}{\dfrac{L}{\left[2Dk_o\int_0^{C_o} g(\alpha)d\alpha\right]^{1/2}} - \dfrac{1.2E_a(-\Delta H)L(1-\gamma)^{1/2}}{2hR_gT_o^2}} \tag{E}$$

$$T_s/T_o = 1 + \frac{(-\Delta H)\epsilon k_o g_o L}{hT_o} \tag{F}$$

$$\begin{cases} k_o = k_{oo}\exp(-E_a/RT_o) \\ (k_p)_s = k_{po}(-E_p/RT_s) \end{cases} \tag{G}$$

$$-\frac{dT_c}{dz} = \frac{\mathcal{U}a}{(\rho C_p)_c}\tau_c(T_o - T_c) \tag{H}$$

TABLE 1B. DESIGN EQUATIONS FOR PLUG-FLOW REACTORS: PORE-MOUTH POISONING AND DIFFUSION LIMITATION

Nonadiabatic, Nonisothermal Reactors

Use Eqs. A, B, E and F of Table 1A for the profiles of C_o, T_o, ϵ and T_s at $t = 0$ ($\gamma = 0$). Based on these initial profiles, proceed with the equations given below

$$C_o - C_c = \left(\frac{L\gamma}{D}\right)\sqrt{2Dk_o}\left[\int_0^{C_c} g(\alpha)d\alpha\right]^{1/2}\exp\left\{\left(\frac{E_a}{2R_gT_o}\right)\frac{(-\Delta H)D(1+B_h\gamma)(C_o-C_c)}{hT_o\gamma + (1+B_h\gamma)(C_o-C_c)(-\Delta H)D}\right\} \tag{A}$$

$$(C_o)_i = (C_o)_{i-1} - \frac{\tau D}{L^2}\Delta z\,\{(C_o)_{i-1} - (C_c)_{i-1}\} \tag{B}$$

$$T_o = T_{in} - \left(\frac{\Delta H}{\rho C_p}\right)(C_o - C_{in}) + \frac{(\rho C_p)_c}{\rho C_p}\frac{\tau}{\tau_c}[(T_c)_{in} - T_c] \tag{C}$$

$$N_o = (N_o)_{in}\exp\left\{\frac{-(k_p)_c\tau z}{1+(\phi_p)_c^2\gamma}\right\} \tag{D}$$

$$\gamma_j = \gamma_{j-1} + \Delta t\left[\frac{(k_p)_c}{Q}\left(\frac{N_o}{1+(\phi_p)_c^2\gamma}\right)\right]_{j-1} \tag{E}$$

$$\epsilon = \frac{D(C_o - C_c)}{k_o g(C_o)L^2\gamma} \tag{F}$$

$$T_s/T_o = 1 + \frac{(-\Delta H)\epsilon k_o g(C_o)L}{hT_o} \tag{G}$$

$$T_c/T_o = 1 + 1 + (B_h\gamma)(T_s/T_o - 1) \tag{H}$$

$$\begin{cases} k_o = k_{oo}\exp(-E_a/RT_o) \\ (k_p)_c = (k_p)_o\exp(-E_p/RT_c) \end{cases} \tag{I}$$

$$-\frac{dT_c}{dz} = \frac{\mathcal{U}a}{(\rho C_p)_c}\tau_c(T_o - T_c) \tag{J}$$

Equation 31 is used instead of Eq. 35 at time zero, since $\gamma = 0$ at that point. The full set of equations for the adiabatic case is given below:

$$(C_o)_i = (C_o)_{i-1} - \frac{\tau D}{L^2\gamma}\Delta z[(C_o)_{i-1} - (C_c)_{i-1}] \tag{36}$$

$$C_o - C_c = \left(\frac{L\gamma}{D}\right)\sqrt{2Dk_o}\left[\int_0^{C_c} g(\alpha)d\alpha\right]^{1/2}\exp\left\{\left(\frac{E_a}{2R_gT_o}\right)\times\left[\frac{(-\Delta H)D(1+\mathrm{Bi}_h\gamma)(C_o-C_c}{hT_oL\gamma + (1+\mathrm{Bi}_h\gamma)(C_o-C_c)(-\Delta H)D}\right]\right\} \tag{25}$$

$$T_o = T_{in} - \left(\frac{-\Delta H}{\rho C_p}\right)(C_o - C_{in}) \tag{37}$$

$$N_o = (N_o)_{in}\exp\left[\frac{-(k_p)_c\tau z}{1j+(\phi_p)_c^2\gamma}\right] \tag{34}$$

$$\gamma_j = \gamma_{j-1} + \Delta t\left[\frac{(k_p)_c}{Q}\left(\frac{N_o}{1+(\phi_p)_c^2\gamma}\right)\right]_{j-1} \tag{38}$$

Equations 36 and 38 are the Euler versions of Eqs. 35 and 9b, respectively. Subscripts i and j denote grid points in space and time. For nonadiabatic reactors, addition of Eq. 4 and replacement of Eq. 37 by 33 completes the set.

The solution procedure in this case is not difficult, but is clearer if we recognize at the outset that Eq. 37 is an auxiliary equation for Eq. 25 and Eq. 34 the same for Eq. 38. For a given time, then, the simultaneous solutions of Eqs. 36 and 25 yields the concentration profile in the reactor. Proceeding to the next time interval, $t + \Delta t$, Eq. 38 is solved for the new γ profile which is then substituted into Eqs. 36 and 25. Simultaneous solution of these then yields the new concentration profile. As indicated earlier, the initial concentration profiles are obtained from Eq. 31. To start the solution, from these profiles at $t = 0^+$ the $N_o(z)$ profile is computed from Eq. 34 and in turn inserted in Eq. 38 for the γ profile at time $(0^+ + \Delta t)$. Simultaneous solution of Eqs. 36 and 25 is then carried out as described above, and the procedure repeated until the final time of interest is attained. This method is also summarized in Table 1.

TABLE 2. PARAMETERS FOR THE MODEL REACTION SYSTEM

$$r(C,T) = kg(C) = k\left(\frac{C}{1 + \xi C}\right)$$

$$k = \exp\left(-\frac{12{,}000}{T} + 14.6\right) \quad (1/s),\ E_a = 23.76 \text{ kcal/mol}$$

$$\xi = \exp\left(\frac{3{,}600}{T} + 3.86\right) \quad (\text{cm}^3/\text{mol})$$

T_{in} varied

$C_{in} = 1.81 \times 10^{-5}$ mol/cm^3

$B_m = 2{,}500$, $D = 10^{-3}$ cm^2/s, $L = 1$ cm, $kg = 2.5$ cm/s

$$\left(\frac{-\Delta H}{\rho C_p}\right) = 4 \times 10^7 \text{ K-cm}^3/\text{mol}$$

$h = 3.245 \times 10^{-4}$ cal/s-cm^2-K

[$\phi_1 = 6.3$ at the reactor inlet]

$(N_o)_{in} = 5 \times 10^{-8}$ mol/cm^3

$Q = 10^{-4}$ mol/cm^3 cat. pellet

$$k_p = \exp\left(-\frac{7{,}000}{T} + 3.27\right), \quad E_p = 13.86 \text{ kcal/mol}$$

$D_p = 10^{-3}$ cm^2/s

τ: varied

$B_h = 40$

Solution of the Design Problem. The solution of the overall design problem posed in Eqs. 1 to 13 can now be obtained using the methodology outlined above. We obtain the values of J corresponding to different choices of τ, given the limit on conversion (i.e., t_f) below which the catalyst is either regenerated or replaced. Thence one may select the value of τ for maximum J. Depending on limitations placed on the reactions, a maximum may not be attained in the sense of $dJ/d\tau = 0$, however the results will clearly reveal any trends present.

EXAMPLES

The procedures developed here have been applied to the model reaction system detailed in Table 2 for an adiabatic reactor. Now a typical limitation on adiabatic reactor operation is that the catalyst temperature should not exceed a certain limit, which normally implies that the inlet temperature is not a free variable for a given inlet concentration. In our example a limit of 1,184 K was imposed on maximum catalyst temperature, and a final conversion limit of 29.6% was used (below which the catalyst would be regenerated). For uniform deactivation the values of J corresponding to a range of τ are shown in Figure 1. The solid line is the J value normalized with respect to that corresponding to τ of 15 seconds. The dotted line is the value of J_m:

$$J_m = (C_{in} - C_{out})/\tau \qquad (39)$$

This quantity is the equivalent of Eq. 1 when there is no catalyst deactivation. Inlet temperatures given in the second column of Table 3 were used for the corresponding τ values. It is seen that the maximum in J for the deactivating reactor occurs at the boundary of highest τ, while exactly the opposite occurs for the case of no deactivation. From a design point of view, then, ignoring catalyst deactivation would lead to the wrong conclusion concerning relative reactor sizes. Since the criterion of Eq. 1 is on the same fixed costs basis (reactor volume), it can also be used to determine, for instance, whether it is better to use two in parallel, each of 15 seconds, or one of 30 seconds. From the figure it follows that the latter should be preferred since it would give a total of (1.4×30) units whereas the former would give a total of $(1 \times 15 \times 2)$ units.

The inlet temperature, outlet concentration at time zero and the duration of a run before regeneration are given in Table 3 for the range of τ considered. As shown in the table, larger reactor size

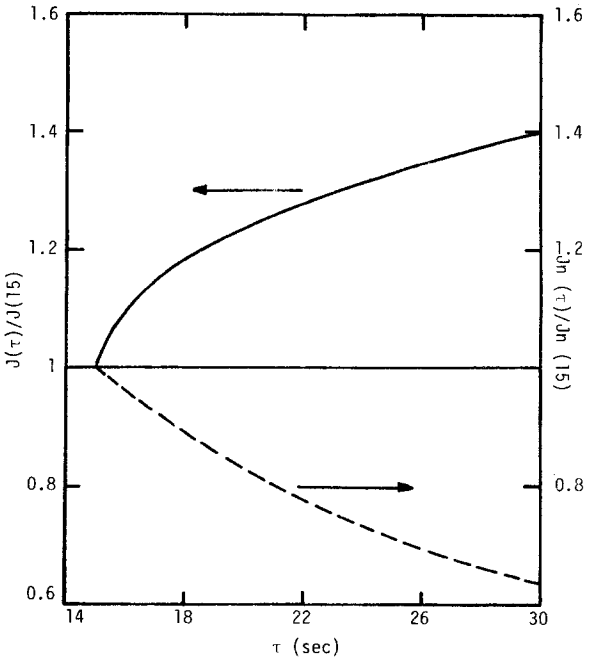

Figure 1. Comparison of performance indices.

gives higher initial conversion and is more tolerant of deactivation, resulting in larger run lengths for the limitations taken to pertain.

Similar conclusions can be made for adiabatic operation and pore-mouth deactivation—calculations again based on the model system set forth in Table 2. Some important design rules also emerge from this analysis, particularly with regard to the very dynamic situation in initial operation shown in Figure 2. A very rapid initial change in conversion is followed by an almost linear decrease with time, and the conversion level reached in this linear range is determined by reactor size. This observation is further supported in Figure 3, where the constraint of catalyst maximum temperature (1,184 K) has been removed. Whatever the initial temperature may be, the conversion moves rather quickly to the same eventual level. We conclude thus that the conversion level in this linear region is largely dictated by reactor size and therefore the initial inlet temperature may be set as high as the maximum temperature constraint will allow.

It is, of course, not surprising that increasing reactor size is in some measure a way to cope with deactivation, since one provides a larger catalyst capacity for the poison, other things considered the same. Nonetheless, a quantitative definition is of importance. Further, the simulation results obtained in solving the overall problem reveal some interesting features. As shown in Figure 4, for uniform deactivation the profile of reactor point effectiveness

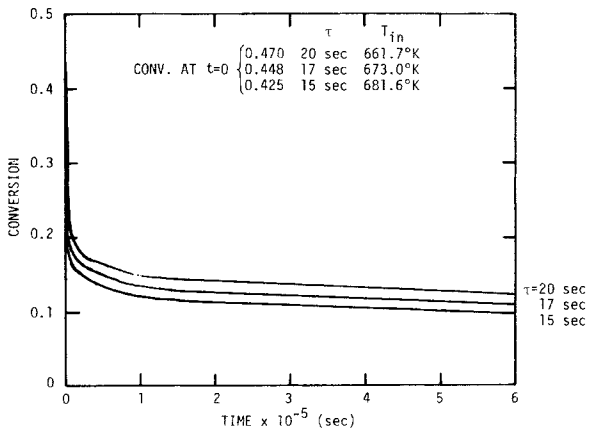

Figure 2. Time behavior of exit conversion with a constraint on maximum catalyst temperature.

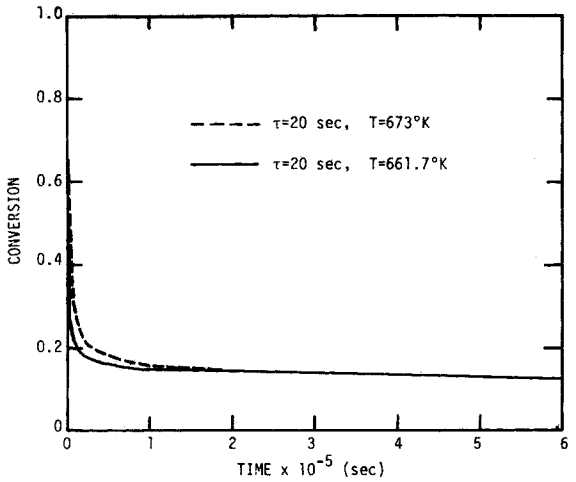

Figure 3. Time behavior of exit conversion with no constraint.

does not change significantly with time. This is the result of compensating effects between the fraction of catalyst deactivated and the internal effectiveness factor, since the latter increases as activity declines. An unusual feature has been observed when the deactivating species is almost completely consumed before reaching the reactor outlet. In such cases the profile of fraction of catalyst deactivated passes through a maximum as shown in Figure 5. The important consequence of this from a design viewpoint is that the maximum catalyst temperature *also* can pass through a maximum with time-on-stream. This is illustrated in Figure 6. Thus, fresh catalyst designs run a good risk of exceeding any temperature constraints. The maxima in the deactivation profiles is the result of interaction between temperature and concentration profiles in the reactor. At the entrance even though the concentration of poison may be high the temperature is (relatively) low and the rate of deactivation is low. As the temperature increases along the adiabatic reaction front, the rate of deactivation is much increased. Depletion of poison accounts for the fall-off in fraction deactivated in the immediate vicinity of the bed exit. As time-on-stream increases, however, there is a diminished uptake of poison in the front of the reactor and correspondingly higher concentrations "leftover" at the bed exit and the maximum tends to move out the end of the bed (cf., $t = 19 \times 10^4$ s, Figure 5). Blaum (1974) has also reported rather unusual reactor profiles resulting from uniform deactivation.

The most important aspect of the behavior described above is the time progression of the outlet catalyst temperature shown in

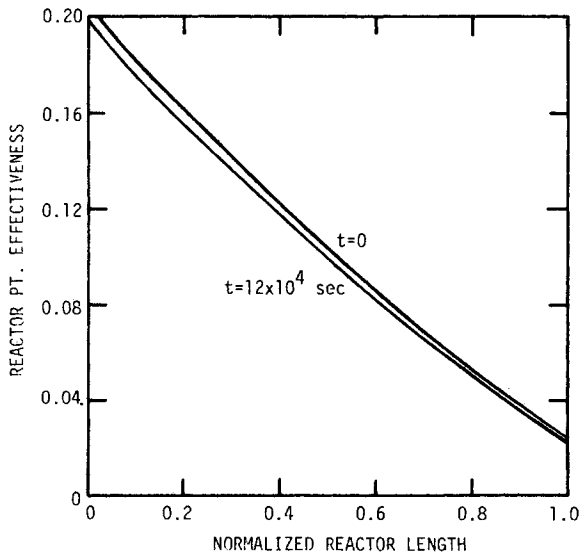

Figure 4. Reactor profiles of reactor point effectiveness, τ = 17 s, uniform deactivation.

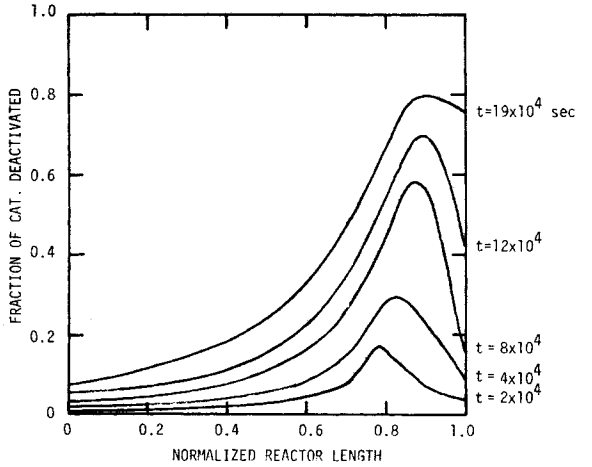

Figure 5. Reactor profiles of fraction of catalyst deactivated, τ = 20 s, uniform deactivation.

Figure 6, together with the exit gas temperature and observed rate. It is seen that the catalyst temperature decreases initially with time, but then is followed by a period during which the temperature is higher than the initial adiabatic maximum catalyst temperature, i.e., the outlet temperature at time zero. Hence, incorrect conclusions may be arrived at on the maximum catalyst temperature allowed if the design consideration is solely based on the behavior at time zero or for fresh catalyst. Usually, the catalyst temperature decreases monotonically with the time on stream. Note also in Figure 6 that the gas temperature *decreases* monotonically with time, in sharp contrast with the behavior of catalyst temperature. The reasons why the temperatures behave as they do are concerned with the fact that the gas temperature is determined by the conversion and yet the rate of heat transfer across the fluid-pellet interface depends on the observed rate of reaction:

$$T_o - T_{in} = \frac{(-\Delta H)}{\rho C_p}(C_{in} - C_o) \tag{37}$$

$$h(T_s - T_o) = (-\Delta H)RL = (-\Delta H)\epsilon k_o(T_o)g(C_o)L \tag{10}$$

where $T_s = T_{cat}$. Since the outlet concentration increases with increasing time, the bulk gas temperature should decrease with increasing time according to Eq. 37. Equation 10 shows that a higher observed rate of reaction $R(= \epsilon k_o g_o)$ results in a higher temperature difference. Therefore, if the rate of decrease of T_o with time is smaller than the rate of increase of R, the catalyst temperature T_s increases with increasing time. The relative magnitudes of these rates then determine whether catalyst temperature increases or decreases with time. In Figure 6 the rate of decrease of T_o is smaller than that of increase of R during the period in which the catalyst temperature is increasing with time. Therefore, there exists a period during which the catalyst temperature is higher than the initial value. This has been observed experimentally (Price and Butt, 1977).

For pore-mouth deactivation similar observations have been made when the concentration of the poisoning species is depleted toward the reactor outlet. In fact, the peak is much sharper than for the case of uniform deactivation, a result we ascribe to different temperature dependencies of γ in the two cases. While γ should

TABLE 3. PERFORMANCE OF THE MODEL REACTOR: UNIFORM POISONING (CONDITIONS GIVEN IN TABLE 2)
Maximum Catalyst Temperature Allowed = 1,183 K
Minimum Conversion Allowed = 29.6%

τ (s)	C_{out} at $t = 0$ (mol/cm^3)	T_{in} (K)	$t_f \times 10^{-5}$ (s)
15	1.043×10^{-4}	681.6	7.00
17	1.007	673.0	8.65
20	0.962	661.8	11.00
23	0.924	652.2	13.38
30	0.846	644.2	18.80

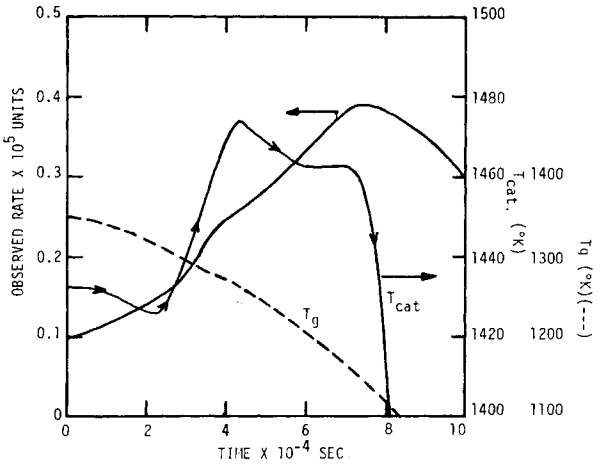

Figure 6. Time profiles of observed rate ($\epsilon_o k_o g_o$), catalyst temperatuare and bulk fluid temperature at the reactor outlet, τ = 20 s, uniform deactivation.

increase monotonically with local temperature for uniform deactivation, more severe diffusion limitation at higher temperatures [$(\phi_p)_c^2$ term in Eq. 9b] considerably moderates this for pore-mouth deactivation. Therefore, as indicated by Eq. 9b, the fraction of catalyst deactivated is largely determined only by the local concentration of poisoning species at high temperatures, while both factors become important at lower temperatures. Another striking fact gleaned from these simulation results for pore-mouth deactivation is how dependent the ultimate fate of the reactor is on the initial stages of deactivation. This is due to the very rapid changes in pellet effectiveness initially caused by the formation of the completely deactivated outer shell of the pellet. This has been demonstrated experimentally in Part I. The reactor point effectiveness, Figure 7, would show even a much more rapid change with time if it were not for the compensating effect of the temperature at the boundary between fresh inner core and deactivated outer shell, which is higher than the bulk gas temperature. However, it still decreases much faster with time than the corresponding point effectiveness for uniform deactivation shown in Figure 2. A final interesting observation concerns the concentration at the forefront of the deactivated outer shell, C_c. Generally one would think of this as decreasing with reactor length, but in fact it increases in the portion of the reactor beyond the point of maximum γ.

CONCLUSIONS

The examples in the previous section demonstrate some of the improvements possible by accounting for deactivation processes in reactor design. The methodology is efficient and is simple enough to be incorporated into various types of optimization problems. While the detailed design and analysis procedures are developed only in the context of plug flow, the methods can be extended to axial dispersion models (Lee, 1981).

The simulation results reveal some interesting features of reactor operation under deactivating conditions. Very important from a practical standpoint is that the maximum catalyst temperature can increase with time-on-stream. This can happen when there is a local maximum of fraction of catalyst deactivated within the reactor. For pore-mouth deactivation, the initial inlet temperature may be set as high as the constraint on maximum temperature will allow. In all cases increase in reactor volume increases tolerance to the effects of deactivation. This would be expected intuitively, but is here made quantitative.

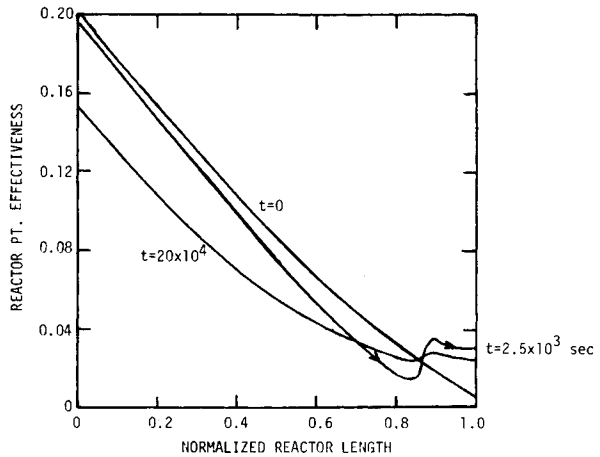

Figure 7. Reactor profiles of reactor point effectiveness, τ = 20 s, pore-mouth deactivation.

ACKNOWLEDGMENT

M. D. Nguyen carried out the simulations for pore-mouth deactivation as a senior project at the University of Florida. J. B. Butt acknowledges the support of the Exxon Educational Foundation.

NOTATION

a = $2/R_t$ (R_t = reactor tube radius)
Bi_h = heat Biot number, $\frac{hL}{\lambda}$
C = concentration of main reactant
C_p = specific heat capacity
D = effective diffusivity of main reactant
D_p = effective diffusivity of poisoning species
E_a = activation energy for main reaction
E_p = activation energy for poisoning reaction
$g(C)$ = concentration dependence of rate of reaction, $r = kg(C)$
h = heat transfer coefficient
$(-\Delta H)$ = heat evolved by main reaction
i = present grid point in z direction
j = present grid point in t direction
J = design performance function given by Eq. 1
k = rate constant for main reaction
k_g = mass transfer coefficient
k_p = rate constant for poisoning reaction
L = characteristic length of pellet, half thickness of slab
N = concentration of poisoning species
Q = poisoning capacity of catalyst in moles poisoning species per pellet volume
r = rate of formation for main reaction
R_g = gas constant
R = global rate for main reaction
R_p = global rate for poisoning reaction
t = time
t_f = final time-on-stream
T = temperature
T_c = coolant temperature
ΔT_d = temperature difference defined in Eq. 20
ΔT_e = temperature difference defined in Eq. 20
U = fluid velocity
$\mathcal{U}$ = overall wall heat transfer coefficient based on mean temperature
x = pellet coordinate
x_c = length of fresh inner core of pore-mouth poisoned pellet
z = reactor coordinate
Z = length of reactor

Greek Letters

α = dummy variable for integration
γ = fraction of catalyst poisoned

ϵ = reactor point effectiveness defined by Eq. 14
ϵ_p = pellet effectiveness
$(\eta_{in})_d$ = effectiveness factor for fresh inner core of deactivated catalyst pellet
η = effectiveness factor for fresh catalyst pellet
λ = thermal conductivity
ρ = density
ϕ_p = Thiele modulus for chemisorption reaction, $L\sqrt{k_p/D_p}$
$(\phi_p)_c$ = $L\sqrt{(k_p)_c/D_p}$
$(\phi_p)_o$ = $L\sqrt{(k_p)_o/D_p}$
τ = residence time, Z/U
τ_c = residence time of coolant
ξ = equilibrium constant in rate expression

Subscripts

c = at $x = x_c$, coolant side
L = at pellet center
p = poisoning species
s = at pellet surface
o = bulk fluid
in = reactor inlet
out = reactor outlet

LITERATURE CITED

Blaum, E., "Zur Dynamik des Katalytischen Festbettreaktors bei Catalysator-desaktivierung-I," *Chem. Eng. Sci.*, **29**, 2263 (1974).

Butt, J. B., D. M. Downing, and J. W. Lee, "Inter-Intraphase Temperature Gradients in Fresh and Deactivated Catalyst Particles," *Ind. Eng. Chem. Fund.*, **16**, 270 (1977).

Carberry, J. J., *Chemical and Catalytic Reaction Engineering*, Chap. 10, McGraw-Hill, New York (1976).

Downing, D. M., J. W. Lee, and J. B. Butt, "Simulation Models for Intraparticle Deactivation: Scope and Reliability," *AIChE J.*, **25**, 461 (1979).

Dumez, F. J., and G. F. Froment, "Dehydrogenation of 1-Butene into Butadiene. Kinetics, Catalyst Coking, and Reactor Design," *Ind. Eng. Chem. Proc. Des. Dev.*, **15**, 291 (1976).

Froment, G. F., and K. B. Bischoff, "Non-steady State Behavior of Fixed-bed Catalytic Reactors Due to Catalyst Fouling," *Chem. Eng. Sci.*, **16**, 189 (1961).

Lee, H. H., "A Criterion of Isothermality And Determination of Reaction Boundary for Pore-mouth Poisoned Catalyst Pellet," *Chem. Eng. Sci.*, **35**, 905 (1980).

Lee, H. H., "An Approximate Approach to Design and Analysis of Heterogeneous Catalytic Reactors," *AIChE J.* **27**, 558 (1981).

Lee, J. W., J. B. Butt, and D. M. Downing, "Kinetic, Transport and Deactivation Rate Interactions on Steady State and Transient Responses in Hetergeneous Catalysis," *AIChE J.*, **24**, 212 (1978).

McGreavy, C., and D. L. Cresswell, "A Lumped Parameter Approximation to a General Model for Catalytic Reactors," *Can. J. Chem. Eng.*, **47**, 583 (1969).

Price, T. H., and J. B. Butt, "Catalyst Poisoning and Fixed Bed Reactor Dynamics—II. Adiabatic Reactors," *Chem. Eng. Sci.*, **32**, 393 (1977).

Weekman, V. W., Jr., "A Model of Catalytic Cracking Conversion in Fixed, Moving, and Fluid-bed Reactors," *Ind. Eng. Chem. Proc. Des. Dev.*, **7**, 90 (1968).

Weng, H. S., G. Eigenberger, and J. B. Butt, "Catalyst Poisoning And Fixed-bed Reactor Dynamics," *Chem. Eng. Sci.*, **30**, 1341 (1975).

Manuscript received October 24, 1980; revision received April 20, and accepted July 14, 1981.

A Study of Fast Tracer Desorption in Molecular Sieve Crystals

JÖRG KÄRGER

Karl Marx University, Leipzig, German Democratic Republic

A modification of the customary NMR (Nuclear Magnetic Resonance) pulsed field gradient technique is shown to allow the observation of tracer desorption phenomena in a time interval of 4 . . . 1 000 ms. The processes observed are only limited by molecular transport in the individual crystallites. Other influences, such as intercrystalline transport resistances and the finite rate of adsorbate supply or adsorption heat dissipation, as known from traditional sorption experiments, can be excluded.

The method is applied to several zeolitic adsorbate-adsorbent systems: methane . . . hexane/NaX; ethane/NaCaA. The tracer desorption curves show the expected dependences on paraffin chain length, sorbate concentration and crystallite size. Comparison with the coefficients of intracrystalline diffusion shows that desorption is limited by intracrystalline transport, excluding the existence of structural surface resistances for these systems. Application of the technique to small zeolite crystallites allows the observation of molecular transport phenomena considerably slower than accessible until now by customary NMR techniques.

SCOPE

The classical method of studying ad- and de-sorption kinetics involves following the transient sorption curve generated when the adsorbent is exposed to a change in ambient sorbate concentration. Besides molecular transport in the individual crystallites, the overall process thus observed may be limited by a number of additional phenomena, such as the intercrystalline transport or the finite rates of adsorbate supply and adsorption heat dissipation. Especially with short sorption times being of the order of or less than 1 s, the latter processes in general completely mask the influence of the microscopic transport. Presented here is a method for recording tracer desorption from

0001-1541-82-5256-0417-$2.00. © The American Institute of Chemical Engineers, 1982.